

Structural Performance of Reinforced Concrete Using 200N/mm² Concrete

Satoru Nagai, Yoshikazu Takaine, Motomi Takahashi & Norio Suzuki
Kajima Technical Research Institute, Japan

Makoto Maruta
Shimane University, Japan



SUMMARY:

Demands for taller structure and wider living space have required reinforced concrete building of a slim and large span structure. Hence we developed an ultra high-strength concrete with a compressive strength as high as 200N/mm². Experiments were carried out to confirm the structural performance of the ultra high-strength concrete members in combination with the world's first ultra high-strength reinforcing steel SD980. It was shown that the ultra high-strength concrete members were able to exhibit an excellent structural performance when appropriate lateral reinforcements were provided. Required strengths were generally evaluated with the conventional design formulas. The spalling of the ultra high-strength concrete observed during early-stage axial loading, a characteristic drawback of this concrete, was resolved by introducing a steel fiber.

Keywords: Ultra High Strength Materials, RC Columns with 200N/mm² Concrete, High Capacity Loading System

1. INTRODUCTION

Several reinforced concrete (RC) high-rise buildings higher than 800m have been recently built overseas. In spite of the frequent earthquakes in Japan, much taller building for housing and more flexible structural systems have been developed. In addition, demands for wider application to RC office building and commercial establishments have required streamlining and large-span structures, and ultra high-strength concrete for RC structure. In this background, application of ultra high-strength concrete column with ultra high-strength concrete of 200N/mm² has been researched in our company.

The size effects have been pointed out in the existing studies of the ultra high-strength concrete members (Kono *et al.* 2008). Specimens used in the existing studies were normally one-fourth scale model due to the limitation of loading apparatus, and the working load at the experiments were generally controlled smaller. However, several new approaches have been made in our research and development that include the material and construction development of the ultra high-strength concrete material of 200N/mm² class, use of the world's first ultra high-strength reinforcing steel, introduction of structural loading apparatus capable of loading 40MN and structural performance evaluation in nearly full-scale. The spalling of the ultra high-strength concrete observed during early-stage axial loading (Kimura and Ishikawa 2001), a characteristic drawback of this concrete, was also addressed.

In this paper, experiments to confirm the structural performance of nearly half-size RC columns using the ultra high-strength concrete of 200N/mm² class and the ultra high-strength reinforcing steel SD980 are presented.

2. ULTRA HIGH-STRENGTH CONCRETE COLUMN TESTS

2.1. Outline

2.1.1. Specimens

The tests comprised the flexural test and the shear test targeted to evaluate flexural strength, deformation capability and shear strength. Specimens for the each tests are shown in Tables 2.1 and 2.2, and the shape and bar arrangements of the specimen are shown in Figs. 2.1 and 2.2.

The specimens were prepared in two sizes: large specimens of nearly half scale model of 450mm square and small specimens with nearly one-fourth scale model of 200mm square. Steel fibers were mixed in concrete to prevent the cover concrete from spalling and the ultra high-strength reinforcing steel SD980 was adopted for the main reinforcements.

The flexural test specimens were eight large specimens with a shear span ratio of 1.5 and the test parameters were the grade of lateral reinforcement (SD1275 or SD785), the lateral reinforcement ratio ($p_w=0.90\text{-}1.63\%$), shape (■ or □ type) and loading method (constant or variable axial load). Among eight specimens, two were assumed to be the inside columns subjected to a constant axial load of 0.3cNu (cNu: Compressive strength of the column) while the other six specimens were assumed to be the peripheral columns subjected to variable axial loads from 0.75tNu to 0.7cNu (tNu: Tensile strength of the column) making it possible to evaluate the structural performance of the ultra high-strength concrete members with a strength of 200N/mm² class not only for the long-term axial strength but also the variable axial loads during earthquakes.

The shear test specimens were eight small-size specimens with a shear span ratio of 1.0 and two large specimens with a shear span ratio of 1.25, and the test parameters were the lateral reinforcement ratio (0.3-0.9%), working axial load of 0.3cNu (hereafter low axial load) or 0.6cNu (hereafter high axial load), with or without steel fiber and the scale of the specimens. Effects of the parameters on the shear cracking strength and the shear strength were examined in the shear test.

2.1.2. Loading Methods

Experimental apparatus including the loading equipment for the large and small-size specimens is shown in Figs 2.3(a) and (b). Both large and small-size specimens were subjected to lateral forces under constant or variable axial forces by the respective loading apparatus undergoing an moment at both ends of the column.

Table 2.1. Specimens of Flexural Test

Specimen	Axial Force ¹⁾	Longitudinal Bar [$f_y(N/mm^2)$] ²⁾	Lateral Bar			Concrete	
			Steel Grade [$f_{wy}(N/mm^2)$] ²⁾	Space(mm) [$p_w(\%)$]	p_{wfwy} (N/mm ²)	Comp. Strength (N/mm ²)	Young's Modulus (kN/mm ²)
U09-C	0.3cNu	24-D19 SD980	U9.0 SBPD 1275	@63 [0.90]	11.8	216	46.7
U14-C				@42 [1.35]	17.7	207	46.9
U09-V	-0.75tNu	[1106]		@63 [0.90]	11.8	212	49.6
U12-V	-0.75tNu 0.2cNu	[1313] except below around bar [1399]		@47 [1.20]	15.8	208	48.2
U14-V				@42 [1.35]	17.7	212	48.1
UR14-V				[1399]	17.8	204	47.9
U16-V	0.7cNu	[1092] U12-V UR14-V		@35 [1.63]	21.4	211	48.5
H16-V			D10 SD785 [902]	@39 [1.63]	14.7	212	48.6

1) cNu = $0.85\sigma_B(bD - \Sigma A_g) + \Sigma A_g f_y$, tNu = $\Sigma A_g \sigma_y$, b, D : Section width and depth,

σ_B : Compressive Strength of Concrete, A_g : Total Section of Longitudinal Bars,

f_y : Yield Strength of Longitudinal Bar

2) Yield Strength of bar according to 0.2% Offset method

Table 2.2. Specimens of Shear Test

Specimen	Section $b \times D$ (mm)	Fiber Type	Axial Force ¹⁾	Longitudinal Bar [$f_y(N/mm^2)$] ²⁾	Lateral Bar			Concrete	
					Steel Grade [$f_{wy}(N/mm^2)$] ²⁾	Leg number, Space(mm) [p_w]	p_{wfwy} (N/mm ²)	Comp. Strength (N/mm ²)	Young's Modulus (kN/mm ²)
U03s-C_1	200 × 200	Steel	0.3cNu	8-D19 SD980 [1106]	2 - @65[0.3%]	4.0	207	46.9	
U045s-C_1			0.3cNu		3 - @65[0.45%]	6.0	188	47.5	
U06s-C_1		-	0.6cNu		3 - @49[0.6%]	8.0	197	45.8	
U09s-C_1			0.3cNu		3 - @33[0.9%]	12.0	197	46.3	
U045s-06C_1	450 × 450	Steel	0.3cNu	24-D19 SD980 [1313]	3 - @65[0.45%]	6.0	198	45.8	
U09s-06C_1			0.6cNu		3 - @33[0.9%]	12.0	200	47.0	
N-U03s-C_1		-	0.3cNu		2 - @65[0.3%]	8.7	203	47.0	
N-U06s-C_1			0.3cNu		3 - @49[0.6%]	6.5	203	46.3	
U045-C_1.25	450 × 450	Steel	0.3cNu	U9.0 SBPD1275 [1313]	4 - @125[0.45%]	5.9	200	47.6	
U045-06C_1.25			0.6cNu			5.9	205	46.6	

1) cNu = $0.85\sigma_B(bD - \Sigma A_g) + \Sigma A_g f_y$, tNu = $\Sigma A_g \sigma_y$, b, D : Section width and depth, σ_B : Compressive Strength of Concrete, A_g : Total Section of Longitudinal Bars, f_y : Yield Strength of Longitudinal Bar

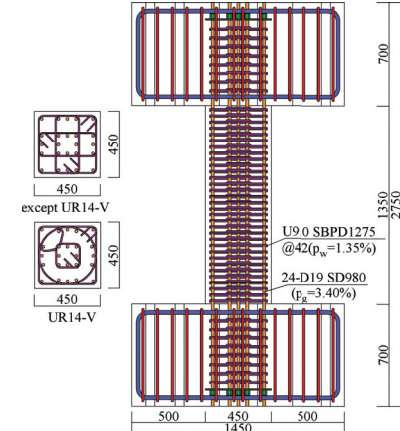


Figure 2.1. Shape and bar arrangement of large-size specimen

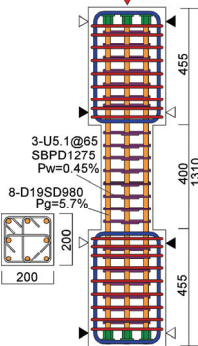


Figure 2.2. Shape and bar arrangement of small-size specimen

The loading method of the lateral forces comprised one cycle of the rotation angle $R=1.25 \times 10^{-3}$ rad and two cycles of 2.5, 5, 10, 20, 30 and 40×10^{-3} rad, which was common to all the specimens. When the peripheral column specimens were subjected to the flexural test, the loading method with variable axial forces according to the changes in bending moment was adopted as shown in Fig. 2.4.

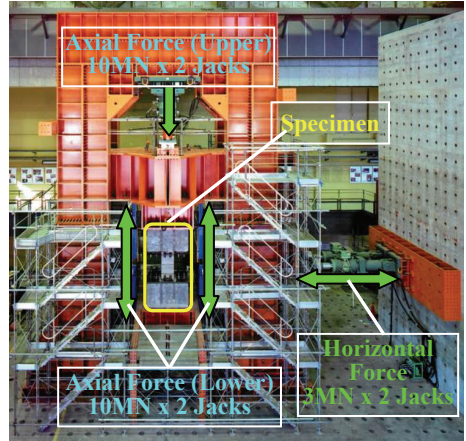
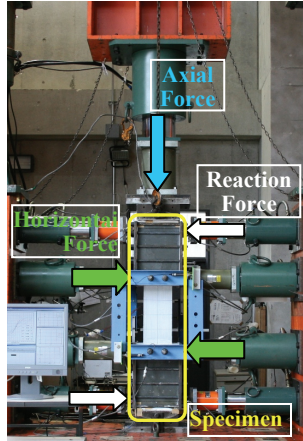


Figure 2.3(a). Loading apparatus for large-size specimens



(b). Loading apparatus for small-size specimen

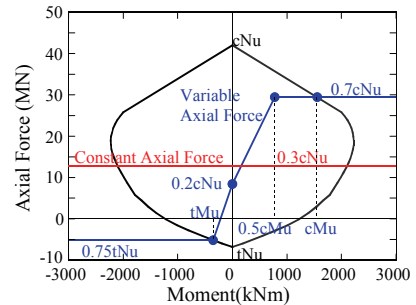


Figure 2.4. Moment-axial force relationship

2.2. Test Results

Results of the flexural and shear tests are shown in Tables 2.3 and 2.4. An example of the relationships between shear force Q and rotation angle R taking account of the $P-\Delta$ effects are shown in Figs. 2.5 and 2.6. Typical damages are shown in Figs. 2.7 and 2.8. Numerical estimation of the flexural strength $ACI Q_{fu}$ according to ACI Building Code Requirements for Structural Concrete and Commentary (ACI 2003) and the shear strength uQ_{su} according to AIJ Design Guideline for Earthquake Resistant Reinforced Concrete Buildings Based on Ultimate Strength Concept (AIJ 1990) are shown in Tables 2.3 and 2.4. The CEB formula was adopted for the effective concrete strength when calculating the uQ_{su} (AIJ 1999). The calculated bond strength Q_{bu0} ($R_p=0$, R_p : inelastic rotation angle in hinge region) according to the AIJ Design Guideline for Earthquake Resistant Reinforced Concrete Buildings Based on Inelastic Displacement Concept (AIJ 1999) and the calculated shear crack strength cQ_{sc} according the principal stress formula (AIJ 1999) are also shown in Tables 2.3 and 2.4. The $ACI Q_{fu}$ is also shown in Fig. 2.5 and the $ACI Q_{fu}$, cQ_{sc} , uQ_{su} are shown in Fig. 2.6.

2.2.1. Flexural Test

The failure processes under compressive axial loads were not different by specimen. The shear strength decreased on a temporary basis associated with the crushing of the cover concrete but increased afterwards with an increase in strain of the lateral reinforcements. After the crushing of the main reinforcements and core concretes, the maximum strength was observed when the lateral reinforcements nearly reached the yield strain. After the maximum strength, the crushing of the core concrete developed and the shear strength was decreased. On the other hand, circular cracks perpendicular to the member axis were developed under the axial tensile force leading to the tensile yield of the main reinforcement, while the shear strength showed no apparent decrease and the specimen indicated no failure.

The decrease in shear strength on a temporary basis associated with the crushing of the cover concrete occurred in the inside and peripheral columns at a rotation angle of $R=10 \times 10^{-3}$ rad and $R=5 \times 10^{-3}$ rad respectively and was at most 300kN. The spalling of the cover concrete was not observed for all the specimens and the validity of steel fibers was confirmed.

The envelope curve of the shear strength Q – rotation angle R relation is shown in Fig. 2.9. Both inside and peripheral columns exhibited higher strength with an increase in the lateral reinforcements and smaller reduction in shear strength after the maximum strength demonstrating excellent deformation

capability. Specimens with \blacksquare type arrangement showed larger shear strength than that with \square type arrangement if compared at the same amount of the lateral reinforcement. In spite of the past study that the shear strength of \blacksquare type and \square type reinforcement was identical (Takahashi *et al.* 1986), specimens with \blacksquare type reinforcement, having much amount of the lateral reinforcement, showed better structural performance in this study, probably because the lateral reinforcement mainly works as a restriction of the core concrete under the high axial loading flexural-compression conditions in this experiments.

2.2.2. Shear Test

The failure processes were not different by specimen. After the shear cracking and before the yield of the main reinforcements of the beam, the crushing of the compression strut developed with an increase in the rotation angle and showed maximum strength which was generally greater than the design shear strength.

The difference in the cracking patterns with and without steel fiber is shown in Fig. 2.10 and an example of the development of the maximum shear crack width at each cycle is shown in Fig. 2.11 where the markers with an abrupt drop were due to unloading. The specimens with steel fibers showed a large number of cracks but the development of crack width associated with the increase in deformation was rather small and were able to restrict the spalling of the cover concrete even under the notable crushing of the compression struts. Hence the use of steel fiber was proven to be effective in inhibiting the damages to members such as spalling of the cover concrete and the development of shear crack width.

Table 2.3. List of Flexural Test Result

Specimen	Experiment			Caluculation							
	Maximum Strength		Limit Deform. ¹⁾	Flexural Strength		Shear Strength			Bond Splitting Strength		
	eQ_{max} (kN)	eR_{max} ($\times 10^{-3}$ rad)	eR_u ($\times 10^{-3}$ rad)	ACI Q_{fu} (kN)	$\frac{eQ_{max}}{ACI Q_{fu}}$	uQ_{su0} ($R_p=0$) (kN)	$\frac{eQ_{max}}{uQ_{su0}}$	uQ_{su1} ($R_p=0.01$) (kN)	$\frac{eQ_{max}}{uQ_{su1}}$	Q_{bu0} ($R_p=0$) (kN)	$\frac{eQ_{max}}{Q_{bu0}}$
U09-C	3364	10.0	25.5	3143	1.07	3672	0.92	2703	1.24	2010	1.67
U14-C	3768	29.6	43.3	3029	1.24	4251	0.89	3777	1.00	2161	1.74
U09-V	2453	10.0	11.1	2467	0.99	3659	0.67	2703	0.91	1990	1.23
U12-V	2760	10.0	18.3	2345	1.18	4116	0.67	3623	0.76	1958	1.41
U14-V	3106	20.0	30.7	2463	1.26	4295	0.72	3819	0.81	2182	1.42
UR14-V	2735	13.4	16.9	2295	1.19	4222	0.65	3749	0.73	2001	1.37
U16-V	3364	30.4	32.0	2459	1.37	4512	0.75	3965	0.85	2296	1.46
H16-V	2688	19.3	20.0	2463	1.09	4082	0.66	3463	0.78	2302	1.17

1) The limit deformation was defined as a deformation when strength decreased for a 95 percent of the maximum strength in the relationship between shear strength and rotation angle taking account of the P- Δ effects.

Table 2.4. List of Shear Test Result

Specimen	Shear Cracking			Maximum Strength		Caluculated Flexural Strength		Calculated Shear Strength	
	Exp.	Calculation		Experiment		ACI Q_{fu} (kN)	$\frac{eQ_{max}}{ACI Q_{fu}}$	uQ_{su} ($R_p=0$) (kN)	$\frac{eQ_{max}}{uQ_{su}}$
		eQ_{sc} (kN)	eQ_{sc} (kN)	$\frac{eQ_{sc}}{eQ_{sc}}$	eQ_{max} (kN)				
U03s-C_1	589	499	1.18	709	9.4	1047	0.68	413	1.72
U045s-C_1	489	470	1.04	695	9.2	972	0.71	460	1.51
U06s-C_1	510	484	1.05	833	10.0	1007	0.83	533	1.56
U09s-C_1	486	484	1.00	890	9.1	1007	0.88	659	1.35
U045s-06C_1	585	674	0.87	652	4.2	858	0.76	469	1.39
U09s-06C_1	643	679	0.95	791	5.0	868	0.91	662	1.20
NU03s-C_1	496	492	1.01	592	5.0	1029	0.58	408	1.45
NU06s-C_1	529	492	1.08	712	5.0	1031	0.69	538	1.32
U045-C_1.25	2846	2357	1.21	2848	5.0	3546	0.80	2381	1.20
U045-06C_1.25	3153	3280	0.96	3211	5.0	3505	0.92	2399	1.34

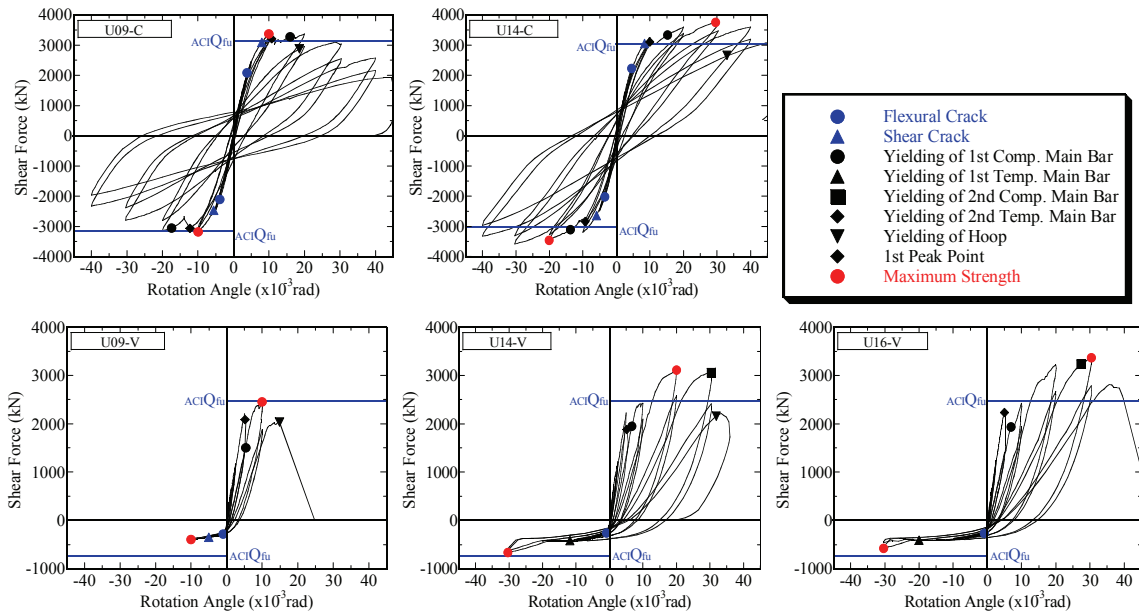


Figure 2.5. Shear force and rotation angle relationships of the flexural test

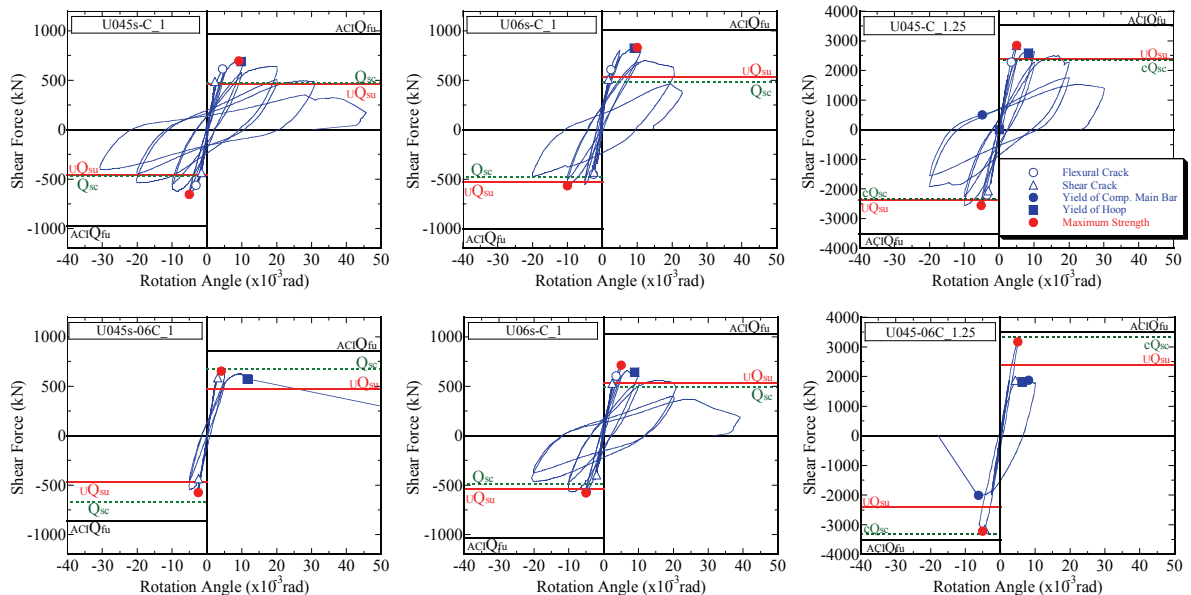


Figure 2.6. Shear force and rotation angle relationships of the shear test

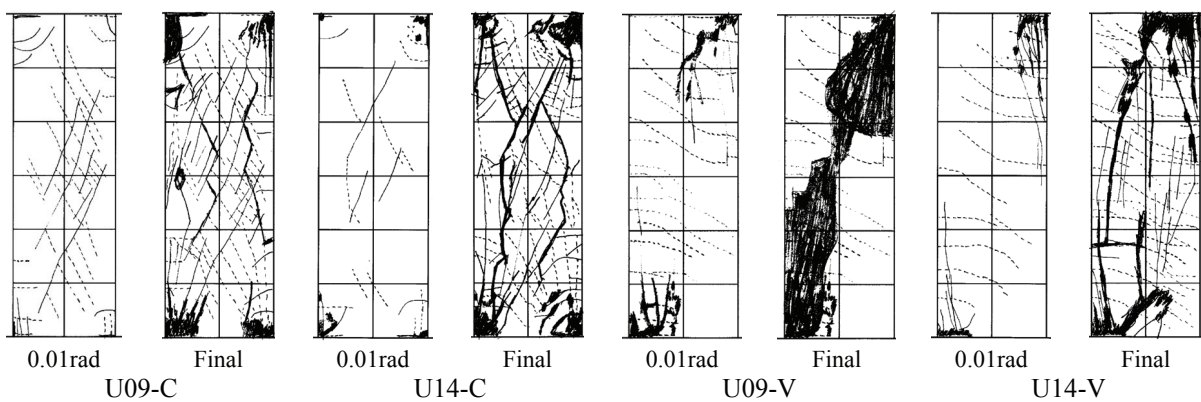


Figure 2.7. Damage condition of the flexural test

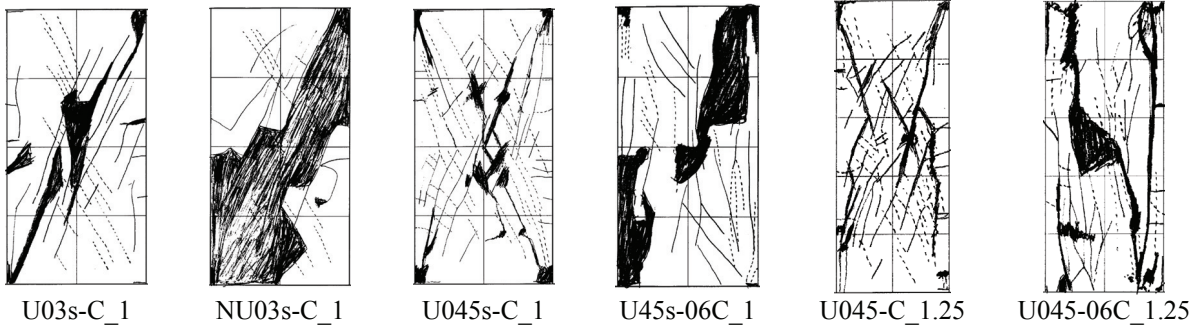


Figure 2.8. Damage condition of the shear test

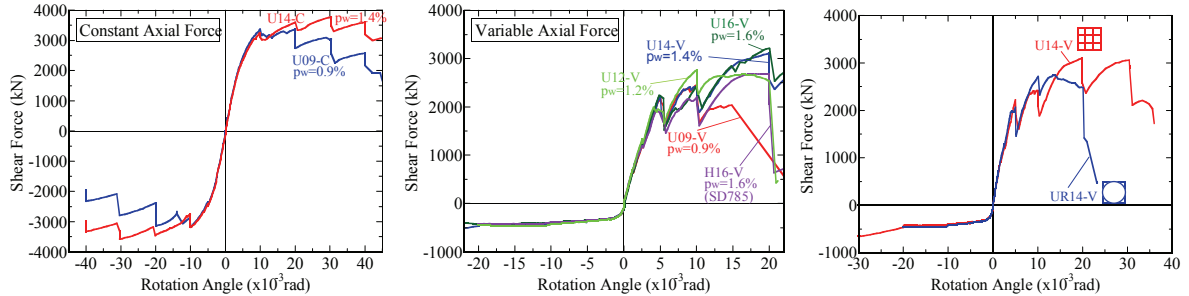


Figure 2.9. Envelope curve of shear force and rotation angle relationships

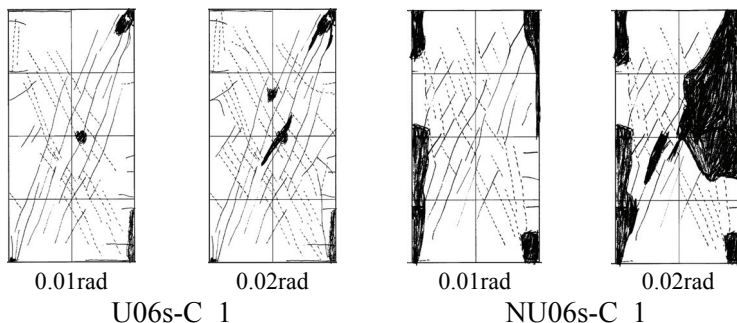


Figure 2.10. Crack patterns

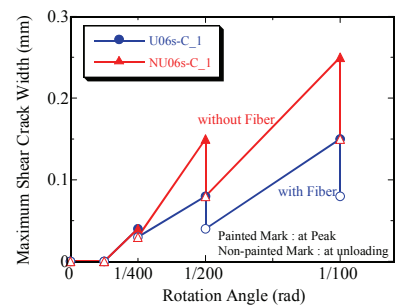


Figure 2.11. Relationship between shear crack width and rotation angle

3. STRUCTURAL PERFORMANCE EVALUATION OF ULTRA HIGH-STRENGTH CONCRETE COLUMN TABLES

3.1. Ultimate Flexural Strength

Relationship between $eQ_{\max}/ACI Q_{fu}$ and $p_w \sigma_{wy}$ is shown in Fig. 3.1, where eQ_{\max} is the maximum strength obtained at the flexural test, $ACI Q_{fu}$ is the flexural strength calculated according to the ACI method and $p_w \sigma_{wy}$ is the amount of the lateral reinforcement.

It is seen for both inside and peripheral columns that the $eQ_{\max}/ACI Q_{fu}$ is generally larger than 1 and the flexural strength may well be evaluated with the ACI method. Also the $eQ_{\max}/ACI Q_{fu}$ tended to increase with an increase in the amount of the lateral reinforcement probably because the core concrete was more restricted with higher amount of the lateral reinforcement leading to an increase in the flexural strength.

3.2. Limit Deformation

Relationship between limit deformation ϵR_u and the amount of lateral reinforcement $p_w \sigma_{wy}$ obtained in the flexural test is shown in Fig. 3.2. The limit deformation was defined as a deformation when

strength decreased for a 95 percent of the maximum strength in the relationship between shear strength and rotation angle taking account of the $P\Delta$ effects.

The limit deformation increased in accordance with an amount of the lateral reinforcement while at the same amount of lateral reinforcement, the limit deformation of the peripheral columns were smaller than that of the inside columns. However, because the limit deformation of the peripheral columns of $p_w=1.4\%$ and 1.6% were nearly identical, the reinforcing limit of the limit deformation was likely to be $p_w=1.4\%$ within the scope of this experiments. When compared at the same amount of lateral reinforcement, the limit deformation of specimen with \blacksquare type reinforcement was larger than that with \square type reinforcement. This is because, as stated above, the \blacksquare type had larger volume of lateral reinforcement that restrained the core concrete more effectively.

3.3. Shear Crack Strength

Relationship between eQ_{sc}/cQ_s and p_w is shown in Fig. 3.3, where eQ_{sc} is the measured shear crack strength obtained in the shear test, cQ_s is the calculated value using the principal stress formula and p_w is the lateral reinforcement ratio. With this result, the shear crack strength can be estimated using the principle stress formula without regard to the scale of the specimen, presence of the steel fiber and working axial forces.

3.4. Shear Ultimate Strength

Relationship between eQ_{max}/uQ_{su} and p_w is shown in Fig. 3.4, where eQ_{max} is the measured shear ultimate strength obtained in the shear test, uQ_{su} is the calculated shear ultimate strength using AIJ ultimate strength formula and p_w is the lateral reinforcement ratio. With this result, the shear ultimate strength can be estimated with the AIJ ultimate strength formula on the safe side. Measured/calculated value of Specimens with the steel fiber was about 20 percent higher than that of specimens without the steel fiber, the contribution of the steel fiber on the shear ultimate strength is implied but needed further research. When the scale of the specimen was different, the measured/calculated values of the

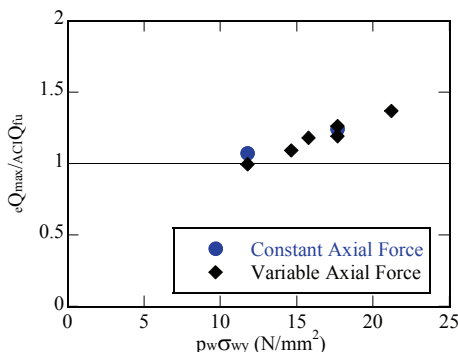


Figure 3.1. Relationship between $eQ_{max}/ACI Q_{fu}$ and $p_w \sigma_{wy}$

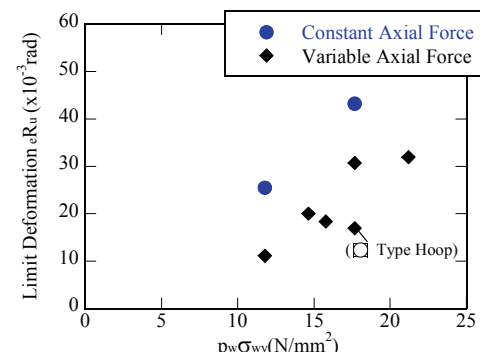


Figure 3.2. Limit deformation

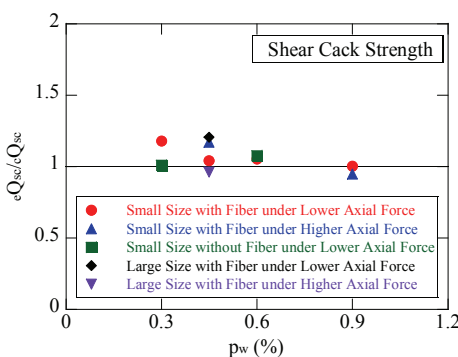


Figure 3.3. Relationship between eQ_{sc}/cQ_{sc} and p_w

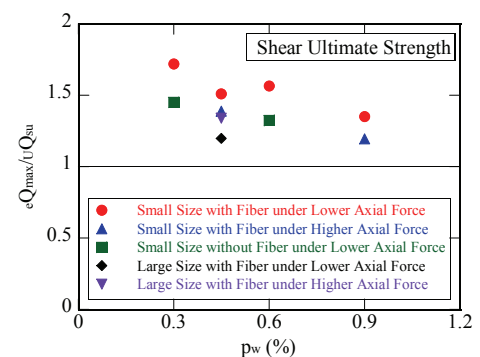


Figure 3.4. Relationship between eQ_{max}/uQ_{su} and p_w

specimens subjected to high axial forces were almost identical but those subjected to low axial forces, the small-scale specimens showed higher strength. This may be attributed to the specimen-scale dependence of tensile force transfer capability of the steel fiber in the shear resistance where it may be large for a small-size specimen and became smaller as the specimen becomes larger.

4. CONCLUDING REMARKS

Experiments of large RC column specimens were carried out to confirm the structural performance of the ultra high-strength concrete columns, with a compressive strength as high as 200N/mm², in combination with the use of ultra high-strength reinforcing steel SD980 for the main reinforcements. The following findings are obtained.

- (1) Spalling of the cover concrete was able to be inhibited by introducing the steel fiber.
- (2) Ultimate flexural strength, ultimate shear strength and shear crack strength was able to be estimated approximately according to the ACI method, the AIJ ultimate strength formula and the principal stress formula respectively.
- (3) Limit deformation generally increased with an increase in the amount of the lateral reinforcement and at the same amount of the lateral reinforcement, the peripheral column specimens subjected to high axial loads showed smaller limit deformation than that of the inside column specimen. Also the limit deformation of the peripheral column showed the upper limit related to the amount of the lateral reinforcement.

As noted above, the ultra high-strength concrete column with a compressive strength of 200N/mm², steel fiber and the ultra high-strength reinforcing steel SD980 for the main reinforcements can express good structural performance provided that an appropriate amount of the lateral reinforcements is assured.

The remaining tasks for the future study include evaluation of hysteresis characteristics, bond strength and fiber-reinforcing effects. In particular, no bond failure was present in this experiments in spite of the measured/calculated value of the bond strength largely exceeded 1.0. This needs to be researched in the future.

REFERENCES

- Architectural Institute of Japan. (1990). Design Guideline for Earthquake Resistant Reinforced Concrete Buildings Based on Ultimate Strength Concept, Architectural Institute of Japan. (in Japanese)
- Architectural Institute of Japan. (1999). Design Guideline for Earthquake Resistant Reinforced Concrete Buildings Based on Inelastic Displacement Concept, Architectural Institute of Japan. (in Japanese)
- American Concrete Institute. (2005). Building Code Requirements for Structural Concrete and Commentary, American Concrete Institute
- Kimura, H. and Ishikawa, Y. (2001). Cyclic Loading Test on RC Columns using Fiber Reinforced High Strength Concrete. *Proceedings of the Japan Concrete Institute* **23: 3**, 211-216. (in Japanese)
- Suzuki, N., Korenaga, T., Ryu, N., Oda, M., Kono, S. and Watanabe, F. (2008). Size Effect of Flexural Capacity of RC Columns Made of High Strength Materials. *Summaries of Technical Papers of Annual Meeting, Architectural Institute of Japan. C-2: STURCTURES IV*, 525-532. (in Japanese)
- Takahasi, W., Matsuzaki, Y., Kobayashi, A., Besho, S., Fukushima, M. and Hatamoto, H. (1986). Shear Capacity of Beams and Columns of High-rise Reinforced Concrete Buildings. Part 2 Ultimate Shear Strength. *Summaries of Technical Papers of Annual Meeting, Architectural Institute of Japan. C: STRUCTURES II*: 167-168. (in Japanese)